

## Electron collision with sulfuryl chloride (SO<sub>2</sub>Cl<sub>2</sub>) molecule

This article has been downloaded from IOPscience. Please scroll down to see the full text article.

2006 J. Phys. B: At. Mol. Opt. Phys. 39 2571

(<http://iopscience.iop.org/0953-4075/39/11/020>)

[The Table of Contents](#) and [more related content](#) is available

Download details:

IP Address: 153.19.42.120

The article was downloaded on 25/12/2008 at 22:09

Please note that [terms and conditions apply](#).

# Electron collision with sulfuryl chloride (SO<sub>2</sub>Cl<sub>2</sub>) molecule

**Czesław Szmytkowski, Paweł Możejko, Stanisław Kwitniewski,  
Alicja Domaracka and Elżbieta Ptasińska-Denga**

Atomic Physics Group, Department of Atomic Physics and Luminescence,  
Faculty of Applied Physics and Mathematics, Gdańsk University of Technology,  
ul. Gabriela Narutowicza 11/12, 80-952 Gdańsk, Poland

E-mail: [czsz@mif.pg.gda.pl](mailto:czsz@mif.pg.gda.pl)

Received 15 March 2006, in final form 23 April 2006

Published 15 May 2006

Online at [stacks.iop.org/JPhysB/39/2571](http://stacks.iop.org/JPhysB/39/2571)

## Abstract

Absolute total cross section (TCS) for electron scattering from sulfuryl chloride (SO<sub>2</sub>Cl<sub>2</sub>) molecules was measured in a linear transmission experiment at energies ranging from 0.5 to 150 eV. The most distinct features found in the TCS are the deep minimum located near 1.8 eV and the broad enhancement peaked around 9.5 eV with a shoulder spanned between 3 and 5 eV. At intermediate energies, the present experimental TCS results agree well with our total cross-section estimations, based on calculations of elastic and ionization cross sections. In addition, the calculated total cross section for SO<sub>2</sub>F<sub>2</sub> is reported. The results for e<sup>-</sup>-SO<sub>2</sub>Cl<sub>2</sub> collisions are compared, for the energy dependence and magnitude, with experimental and computed cross sections for other molecules (SO<sub>2</sub>F<sub>2</sub>, SO<sub>2</sub>ClF) comprising a sulfone group.

(Some figures in this article are in colour only in the electronic version)

## 1. Introduction

Sulfuryl chloride (SO<sub>2</sub>Cl<sub>2</sub>) is a compound of industrial, environmental and scientific interest. This substance is widely used as a chlorinating [1] and/or sulfonating [2] reagent and, it is also considered as a component of the catholyte system in batteries [3]. Recently, SO<sub>2</sub>Cl<sub>2</sub> has been suggested as the minor constituent of the Venus atmosphere where it might play a catalytic role [4].

Studies on the electron-assisted processes involving SO<sub>2</sub>Cl<sub>2</sub> molecules started some decades ago; however, the respective data still remain scarce and fragmentary. To date, experimental works on e<sup>-</sup>-SO<sub>2</sub>Cl<sub>2</sub> reactions concerned just the formation of negative ions [5–8] and/or ionization [6] induced by the electron impact, but derived electron-scattering intensities were reported in arbitrary units only.

The present work is one in a series of our experiments carried out to provide the absolute electron-scattering total cross sections (TCS) from low to intermediate energies for molecules of scientific as well as practical importance. The TCS is an electron-scattering quantity which can be obtained in an absolute scale, within a typical accuracy of 3–10% from low to high impact energies. Due to its summary nature, the TCS contains overall information on the scattering processes. Therefore, the explanation of TCS variation versus energy, especially the origin of its spectacular features, demands complementary data concerning particular scattering channels. Nevertheless, the TCS data alone also give valuable information on the scattering phenomena. Reliable absolute TCS data may be used for rough but reasonable estimations of partial cross sections for targets for which scattering data are not available due to experimental or computational difficulties, and may be used as well for normalization of scattering intensities obtained in arbitrary units. Because the TCS is often the only available absolute electron-scattering intensity, it is particularly useful as a quantitative test of the validity of theoretical models and computational procedures. Additionally, the TCS features indicate energy regions which may be worth of further more detailed investigations. Last but not the least, accurate electron-scattering TCSs are indispensable when studying the role of projectile in the scattering [9].

Moreover, systematic studies on the TCS energy dependences for a series of targets often reveal some regularities in the TCS behaviour when going across the given target family [10–14]. Consequently, the TCS study may give valuable insight into the role of a molecular structure in the scattering dynamics, being the stimulus for theoretical investigations [15]. Indeed, the recent TCS experiments [16–18] have already indicated that the arrangement of atoms in a molecule essentially influences the low-energy TCS behaviour (*isomeric effect*). It was also possible to observe some substitutional effect, e.g. replacing hydrogen atoms in a molecule with fluorine distinctly changes the shape of the TCS low-energy function and strongly increases the cross-section magnitude above the ionization threshold (*perfluorination effect*; cf [18–26]). Most of the aforementioned experiments concerned, however, perhydro- and/or perfluoro-carbons only. Therefore, to look for regularities in another group of molecules our research work has been recently directed towards sulfur-containing species.

As mentioned above, the primary motivation of the present work was to measure absolute total cross sections for scattering of low- and intermediate-energy electrons by  $\text{SO}_2\text{Cl}_2$  molecules. The next goal was to calculate total cross sections for electron scattering from  $\text{SO}_2\text{Cl}_2$  and  $\text{SO}_2\text{F}_2$ . The measured and calculated TCS results for  $\text{SO}_2\text{Cl}_2$  are then compared with experimental and theoretical TCS data for other molecules ( $\text{SO}_2\text{F}_2$  and  $\text{SO}_2\text{ClF}$ ) containing a sulfone group and for  $\text{SO}_2$  as well.

## 2. Experimental procedure

An electron-transmission spectrometer is used for the absolute electron-scattering TCS measurements. The experimental set-up and procedure applied in the present work are in principle almost the same as those used in the series of our recent TCS experiments [13, 27] and therefore are only summarized here. The spectrometer consists of an electron source, an electrostatic  $127^\circ$  cylindrical condenser for energy selection, a system of electrostatic lenses to form an electron beam, a scattering cell followed by a retarding field lens system and a Faraday cup as an electron detector. The detector accepts electrons from within a solid angle of nearly 0.8 msr. Elements of the electron optics are housed in a vacuum chamber at a base pressure of 20  $\mu\text{Pa}$ , which rises to 0.2–1 mPa when a target vapour is admitted. The magnetic field over the whole electron optics volume of the spectrometer is reduced to a value below 0.1  $\mu\text{T}$ . The target vapour, filling up the scattering cell, is irradiated by an electron beam of desired

energy  $E$  ( $\Delta E \sim 0.1$  eV, fwhm). These electrons which emerge from the cell throughout the exit aperture cross the retarding field assembly which prevents inelastically scattered electrons being collected with the Faraday cup.

The total cross section,  $Q(E)$ , is derived from intensities of the transmitted electron currents measured in the presence,  $I(E, p)$ , and absence,  $I(E, p = 0)$ , of the target molecules in the reaction cell, and applying the Bouguer–de Beer–Lambert (BBL) relationship

$$Q(E) = \frac{k\sqrt{T_m T_c}}{pL} \ln \frac{I(E, 0)}{I(E, p)},$$

in which the thermal transpiration effect [28] is accounted for;  $k$  denotes the Boltzmann constant,  $L$  (=30.5 mm) is the electron path length in the scattering chamber,  $p$  stands for the target gas pressure, while  $T_c$  (310–320 K) and  $T_m$  (=322 K) are the temperature of the scattering cell and the temperature of the mks manometer head, respectively. All these quantities are measured directly and therefore the obtained total cross sections are in the absolute scale. Data acquisition and their processing are controlled by a PC.

As a reference for the energy scale, the resonant undulating structure visible at around 2.3 eV when N<sub>2</sub> is admixed is used. A small incremental shift of the energy scale was observed in course of the experiment, probably due to strong reactivity of SO<sub>2</sub>Cl<sub>2</sub> with the electron optics elements. This shift increases the ultimate uncertainty of the electron energy to about 0.12 eV.

Carrying out the measurements, some extra difficulties were encountered related to the presence of SO<sub>2</sub>Cl<sub>2</sub> traces effusing from the scattering cell into the region of filament and electron optics volume. To lessen the influence of the target vapour on the incident electron beam and, in consequence, on the measured TCS, the whole electron optics was first passivated with SO<sub>2</sub>Cl<sub>2</sub>. Then, in the course of the TCS measurements, the target was supplied alternately into the reaction cell and its surrounding in such a way that the background pressure in the region of the filament and electron optics was maintained constant irrespective of whether the target was present in the cell or not. Such a procedure assured independence, within statistical uncertainty, of the incident electron beam and the measured TCS of the applied target pressure (40–200 mPa). To reduce condensation of SO<sub>2</sub>Cl<sub>2</sub> vapours on the electron optics surfaces, their elements were heated to about 315 K. However, an accumulation of SO<sub>2</sub>Cl<sub>2</sub> on the walls of a vacuum chamber (kept at room temperature) noticeably prolonged the evacuation time for the SO<sub>2</sub>Cl<sub>2</sub> vapour and gradually, though slowly, increased the background pressure in the electron optics region. In addition, reactivity of SO<sub>2</sub>Cl<sub>2</sub> with elements of electron optics caused a gradual worsening of the transmission of electrons across the spectrometer. Therefore, after few days of measurements, the cleaning of the electron optics elements was necessary; such a procedure restored properties of the spectrometer to a satisfactory level. The corrosive action of the SO<sub>2</sub>Cl<sub>2</sub> vapour resulted also in unremovable damage of the rotary pump system.

The TCS in every single run is derived from the average of single electron current intensities, 100 taken with and 100 without the target in the scattering cell, and from the respective target pressure readings. The lowering of the electron current transmission during the single run was negligible and did not influence the measured TCS. The final TCS value at each energy is a weighted mean of results from a series (4–10) of individual runs (7–10 in series). The problems mentioned above forced us to reduce the number of series carried out in our typical TCS experiments. Anyway, the statistical uncertainty of the TCS is below 2% over the entire energy range investigated. The systematic uncertainty of our absolute cross sections is a sum of uncertainties related to the forward small-angle scattering, to the factor  $pL$  in the BBL relationship and to the electron intensity readings; the results at low energies,

where the TCS energy function changes steeply, may be charged with an extra uncertainty due to the shift in the energy scale. The overall systematic uncertainty amounts up to 8–10% below 3 eV, decreases gradually to 5% in the energy range of 10–100 eV and reaches again about 7% at higher applied energies.

A commercially supplied sample of SO<sub>2</sub>Cl<sub>2</sub> (liquid of 97% purity from Aldrich) was purified before using it in a series of freeze-pump-thaw cycles to remove air and other impurities volatile at the liquid N<sub>2</sub> temperature. To avoid the influence of possible decomposition of SO<sub>2</sub>Cl<sub>2</sub> into SO<sub>2</sub> and Cl<sub>2</sub> on the measured TCS, after few days the target handling system was cleaned up and refilled with a new portion of the SO<sub>2</sub>Cl<sub>2</sub> probe. The absence of low-energy TCS feature characteristics for SO<sub>2</sub> [29] and those for Cl<sub>2</sub> [30, 31] in the TCS for SO<sub>2</sub>Cl<sub>2</sub> assures us that the decomposition of SO<sub>2</sub>Cl<sub>2</sub> in the target inlet system is not significant in our experiment.

### 3. Methods of calculations

Complementary to the experimental work, we have estimated theoretically the total cross section for electron–SO<sub>2</sub>Cl<sub>2</sub> scattering at intermediate energies, and in addition for a SO<sub>2</sub>F<sub>2</sub> molecule. One of the motivations for calculation of the cross section for SO<sub>2</sub>Cl<sub>2</sub> is that we did not obtain experimental data above 150 eV due to the difficulties we met in course of the e<sup>−</sup>–SO<sub>2</sub>Cl<sub>2</sub> experiment. The need for intermediate-energy total cross-section predictions for SO<sub>2</sub>F<sub>2</sub> comes from two facts: to date, the experimental TCS values for this molecule are not reported above 12 eV and the only available low-energy data [33] are significantly lower than those for a SO<sub>2</sub> molecule [29], which at higher collision energies is rather unusual. The total cross sections calculated for SO<sub>2</sub>Cl<sub>2</sub> and SO<sub>2</sub>F<sub>2</sub> can be compared with recent computations for another member of the family—SO<sub>2</sub>ClF [34]. For discussion and test purposes, we have also calculated ionization (ICS) and elastic cross sections (ECS) for SO<sub>2</sub> for which a more extensive data set of experimental and theoretical cross sections is available (cf [29]). The theoretical approach and computational methods used in the present calculations are nearly the same as those we have used in previous works [34–37]; thus, only a short description of applied procedures is provided here.

The cross sections for electron-impact ionization of SO<sub>2</sub>, SO<sub>2</sub>Cl<sub>2</sub> and SO<sub>2</sub>F<sub>2</sub> molecules at energies ranging from the ionization threshold up to 4000 eV have been computed within the binary-encounter-Bethe (BEB) formalism [38]. According to this approximation, the electron-impact ionization cross section per molecular orbital is given by the relation

$$\sigma^{\text{BEB}} = \frac{S}{t+u+1} \left[ \frac{\ln t}{2} \left( 1 - \frac{1}{t^2} \right) + 1 - \frac{1}{t} - \frac{\ln t}{t+1} \right],$$

where  $S = 4\pi a_0^2 N R^2 / B^2$  ( $a_0 = 0.5292 \text{ \AA}$ ,  $R = 13.61 \text{ eV}$ ),  $u = U/B$ ,  $t = T/B$ , and  $T$  is the energy of the impinging electron. The total cross section for electron-impact ionization (ICS) has been obtained as the sum of  $\sigma^{\text{BEB}}$  for all occupied molecular orbitals. All molecular parameters necessary to compute the ionization cross section within the BEB approach such as the electron binding energy,  $B$ , kinetic energy of the orbital,  $U$ , and orbital occupation number were obtained for the ground states of the geometrically optimized molecules with the Hartree–Fock method using the GAUSSIAN 03 code [39] and the Gaussian 6-311G basis set; as a starting molecular geometry, the experimental values of bond length and angles have been used (see table 3). Because the valence orbital energies obtained this way usually have slightly higher values than the experimental ones, we additionally performed the outer valence Green function calculations of correlated electron affinities and ionization potentials [40], also with the GAUSSIAN 03 code. Obtained this way, the ionization cross section for a SO<sub>2</sub> molecule

(not presented in this paper) agrees well according to the shape and value with published theoretical [41] and experimental [42, 43] ionization data.

Elastic electron-scattering cross sections for SO<sub>2</sub>, SO<sub>2</sub>Cl<sub>2</sub> and SO<sub>2</sub>F<sub>2</sub> molecules, between 30 and 4000 eV, have been calculated with the independent atom method (IAM) [44] with a static and polarization model potential. In this approximation, the integral cross section for elastic electron–molecule scattering is given by

$$\sigma^{\text{EL}}(E) = \frac{4\pi}{k} \sum_{i=1}^N \text{Im} f_i(\theta = 0, k) = \sum_{i=1}^N \sigma_i^{\text{el}}(E),$$

where  $\sigma_i^{\text{el}}(E)$  is the integral elastic cross section of the  $i$ th atom of the target molecule,  $E$  is the energy,  $k = \sqrt{2E}$  is the wave number of the incident electron,  $N$  is the number of atoms within the molecule,  $f_i(\theta, k)$  is the complex scattering amplitude due to the  $i$ th atom of the molecule and  $\theta$  is the scattering angle. The atomic elastic ICS for the  $i$ th atom of the target molecule,  $\sigma_i^{\text{el}}(E)$ , has been computed according to

$$\sigma^{\text{el}} = \frac{4\pi}{k^2} \left( \sum_{l=0}^{l_{\text{max}}} (2l+1) \sin^2 \delta_l + \sum_{l=l_{\text{max}}+1}^{\infty} (2l+1) \sin^2 \delta_l^{(B)} \right).$$

To obtain phase shifts  $\delta_l$ , partial wave analysis has been employed and the radial Schrödinger equation,

$$\left[ \frac{d^2}{dr^2} - \frac{l(l+1)}{r^2} - 2(V_{\text{stat}}(r) + V_{\text{polar}}(r)) + k^2 \right] u_l(r) = 0,$$

has been solved numerically under the boundary conditions

$$u_l(0) = 0, \quad u_l(r) \xrightarrow{r \rightarrow \infty} A_l \hat{j}_l(kr) - B_l \hat{n}_l(kr),$$

where  $\hat{j}_l(kr)$  and  $\hat{n}_l(kr)$  are the Riccati–Bessel and Riccati–Neumann functions, respectively. The electron–atom interaction has been described by a sum of static [45],  $V_{\text{stat}}(r)$ , and polarization [46, 47],  $V_{\text{polar}}(r)$ , model potentials. The phase shifts  $\delta_l$  are related to the asymptotic form of the wavefunction,  $u_l(r)$ , by

$$\tan \delta_l = \frac{B_l}{A_l}.$$

The exact phase shifts have been calculated for  $l$  up to  $l_{\text{max}} = 50$ , while those for  $l > 50$  have been included through the Born approximation. It has been shown that the elastic integral cross section calculated within such an approximation reasonably well reproduces the experimental elastic cross section for electron scattering from polyatomic molecules at collision energies typically above 70 eV [35].

Finally, we have estimated the total cross section for electron scattering from SO<sub>2</sub>, SO<sub>2</sub>Cl<sub>2</sub> and SO<sub>2</sub>F<sub>2</sub> molecules as a sum of the calculated ionization and elastic cross sections. It is worth noting that the approach used in the present work has been recently employed successfully to reproduce the total cross sections for electron scattering from NF<sub>3</sub> [26], SO<sub>2</sub>ClF [34] and SF<sub>4</sub> [37] molecules, at energies above 70 eV.

## 4. Results and discussion

### 4.1. Sulfuryl chloride, SO<sub>2</sub>Cl<sub>2</sub>

Variation of the absolute electron-scattering *grand* total cross section for SO<sub>2</sub>Cl<sub>2</sub> measured in the present experiment at energies ranging from 0.5 to 150 eV is shown in figure 1. The

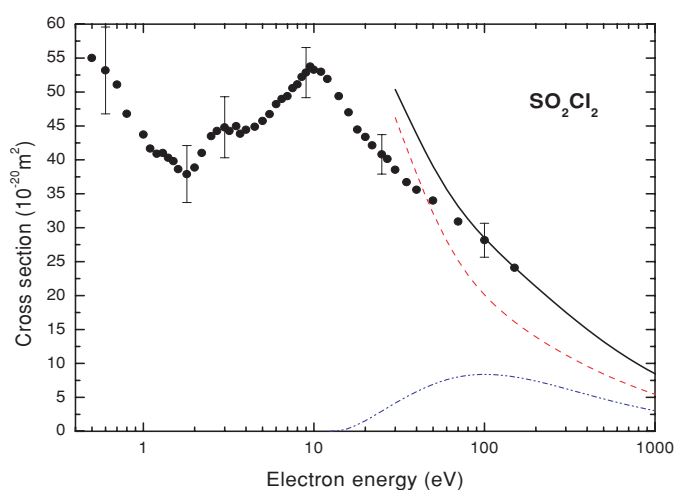


**Figure 1.** Energy dependence of the present (●) experimental  $e^-$ - $\text{SO}_2\text{Cl}_2$  TCS and present calculated cross sections: —, total (elastic + ionization); - - -, elastic (IAM); — · —, ionization (BEB). The error bars at selected points represent the sum of statistical and systematical uncertainties.

**Table 1.** Absolute total cross section (TCS) for electron scattering from sulfuryl chloride ( $\text{SO}_2\text{Cl}_2$ ) molecules in units of  $10^{-20} \text{ m}^2$ .

Energy (eV)	TCS	Energy (eV)	TCS	Energy (eV)	TCS	Energy (eV)	TCS	Energy (eV)	TCS
0.5	55.0	1.6	38.6	4.0	44.4	9.0	52.9	25	40.8
0.6	53.2	1.8	37.9	4.5	44.9	9.5	53.8	27	40.1
0.7	51.1	2.0	38.8	5.0	45.7	10	53.3	30	38.5
0.8	46.8	2.2	41.0	5.5	46.7	11	53.0	35	36.7
1.0	43.7	2.5	43.5	6.0	48.2	12	51.9	40	35.6
1.1	41.7	2.7	44.3	6.5	49.0	14	49.4	50	34.0
1.2	40.9	3.0	44.8	7.0	49.4	16	47.0	70	30.9
1.3	41.0	3.2	44.3	7.5	50.5	18	44.5	100	28.2
1.4	40.3	3.5	44.9	8.0	51.1	20	43.3	150	24.1
1.5	39.8	3.7	43.8	8.5	52.2	22	42.1		

experimental data are compared with the total cross section composed as a sum of elastic integral and ionization cross sections computed in this work, at intermediate energies. The experimental TCS numerical data are listed in table 1 while the calculated cross-section values are available in table 2. We are not aware of any other experimental TCS as well as theoretical cross sections for the  $e^-$ - $\text{SO}_2\text{Cl}_2$  collision.

The most characteristic feature of the measured electron- $\text{SO}_2\text{Cl}_2$  TCS energy dependence is the deep minimum ( $38 \times 10^{-20} \text{ m}^2$ ) located around 1.8–2 eV. Towards lower energies, the TCS increases up to  $55 \times 10^{-20} \text{ m}^2$  at 0.5 eV. Such a steep behaviour of the low-energy TCS is predominantly related to direct scattering of electron projectile in a strong field of a long-range electron-molecule interaction (the permanent electric dipole moment of  $\text{SO}_2\text{Cl}_2$  is relatively high and amounts to 1.81 D; the electric dipole polarizability is  $10.5 \times 10^{-30} \text{ m}^3$  [48]). In a long-distant field of a molecule, the interaction time between the slow impinging electron and the molecule lasts relatively long, which results in the enhancement of the low-energy cross section. A weak shoulder noticeable on the descending TCS curve near 1.2 eV may, however,

**Table 2.** Ionization (ICS) and integral elastic (ECS) cross sections calculated for electron impact on SO<sub>2</sub>Cl<sub>2</sub> molecule (in units of 10<sup>-20</sup> m<sup>2</sup>).

Energy (eV)	ICS	Energy (eV)	ICS	ECS	Energy (eV)	ICS	ECS
12.4	0.00	40	5.84	37.9	250	6.81	12.4
13.0	0.0282	45	6.44	34.8	300	6.28	11.2
14.0	0.0848	50	6.92	32.1	350	5.82	10.3
15.0	0.230	60	7.59	28.1	400	5.42	9.60
16.0	0.428	70	8.00	25.2	450	5.08	8.97
17.0	0.707	80	8.23	23.0	500	4.77	8.43
18.0	0.993	90	8.35	21.4	600	4.26	7.56
19.0	1.275	100	8.39	20.1	700	3.86	6.87
20.0	1.554	110	8.37	19.0	800	3.53	6.31
22.0	2.14	120	8.32	18.2	900	3.25	5.85
25.0	2.97	140	8.14	16.7	1000	3.02	5.46
27.0	3.48	160	7.91	15.6	2000	1.80	3.42
30.0	4.15	180	7.66	14.7	3000	1.30	2.67
35.0	5.09	200	7.41	13.9	4000	1.03	2.41

**Table 3.** A comparison of selected properties for SO<sub>2</sub>-containing molecules (X, Y = F, Cl; cf figure 3); interatomic distances and angles in sulfonyl halides are from [49].

Molecule	Dipole moment (Debye)	Polarizability (10 <sup>-30</sup> m <sup>3</sup> )	Distance (10 <sup>-10</sup> m)			Angle (deg)	
			S—O	S—Cl	S—F	OSO	XSY
SO <sub>2</sub> Cl <sub>2</sub>	1.81 <sup>a</sup>	10.5 <sup>a</sup>	1.418	2.012		123.5	100.3
SO <sub>2</sub> ClF	1.5–1.9 <sup>b</sup>	9.1 <sup>c</sup>	1.409	1.986	1.540	123.3	98.1
SO <sub>2</sub> F <sub>2</sub>	1.12 <sup>a</sup>	6.7 <sup>c</sup>	1.397		1.530	122.6	96.7
SO <sub>2</sub>	1.63 <sup>a</sup>	3.7–4.3 <sup>a</sup>	1.431 <sup>a</sup>			119.3 <sup>a</sup>	

<sup>a</sup> [48].<sup>b</sup> [34].<sup>c</sup> Based on the formula from [50].

be a resonant in the origin. In the resonant channel, the incident electron of energy from an appropriate range attaches temporarily to the target molecule and forms a negative ion for a time interval long compared to the electron passage time. Subsequently, the transient anion can decompose via electron auto-detachment and/or throughout dissociation into the negative fragment and neutral. Evidence for the presence of resonant processes in the region of the 1.2 eV feature comes from experiments [5, 7, 8] in which fragment anions (Cl<sup>-</sup>, Cl<sub>2</sub><sup>-</sup>) were detected between 0.6 and 2 eV, with the narrow peaks centred within 0.9–1.2 eV.

At energies beyond 2 eV the measured TCS starts to increase again. Between 3 and 6 eV, experiments on dissociative electron attachment [5, 7, 8] reveal formation of numerous negative fragment ions (e.g. Cl<sup>-</sup>, Cl<sub>2</sub><sup>-</sup>, SO<sub>2</sub><sup>-</sup>), with the intensities peaked at about 5.1, 4.4 and 5.2 eV, respectively. This suggests that the resonant processes contribute noticeably to the scattering around 4–5 eV, which reflects as the distinct shoulder visible between 3 and 5 eV on the rising left-hand slope of the TCS function. The pronounced TCS enhancement peaks near 9.5 eV with the value of  $54 \times 10^{-20}$  m<sup>2</sup>. A more thorough inspection of the maximum vicinity reveals another weak (but repetitive) structure located near 12 eV. Such features, near 10 eV, are probably the common behaviour of molecules with external chlorine atoms (cf [13, 31, 32]) and are in part related to resonant effects. Therefore, we suggest that the peak at 9.5 eV and the shoulder near 12 eV may be connected with the formation of Cl<sup>-</sup> ions via dissociative electron attachment and dissociative ionization as well. Based on the results for

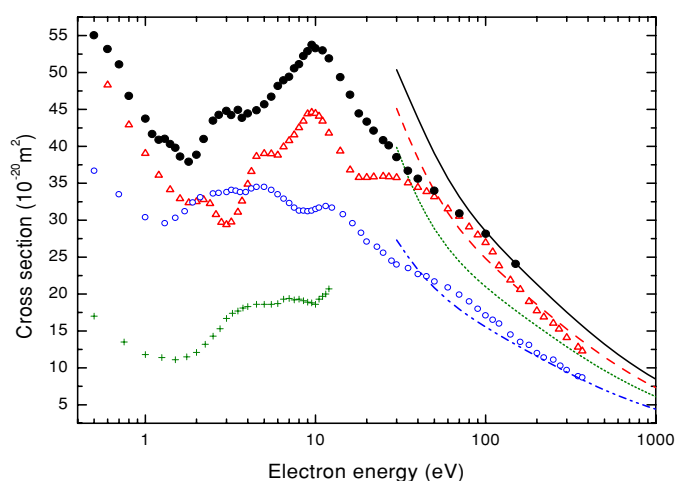


**Figure 2.** A comparison of electron-scattering total cross sections for some sulfur-containing molecules. Experimental TCS: ●, SO<sub>2</sub>Cl<sub>2</sub>, present; △, SO<sub>2</sub>ClF, [34]; +, SO<sub>2</sub>F<sub>2</sub>, [33]; ○, SO<sub>2</sub>, [29]. Theoretical TCS (present): —, SO<sub>2</sub>Cl<sub>2</sub>; ·····, SO<sub>2</sub>F<sub>2</sub>; — · —, SO<sub>2</sub>; and - - - -, SO<sub>2</sub>ClF [34].

targets for which electron-scattering processes are known much better, one may suppose with high certainty that the main contribution to the TCS in the region of the broad enhancement comes from elastic direct scattering although some inelastic direct and resonant processes are also possible. Further speculation on the share of different processes in the TCS enhancement range is an arduous task and almost impossible to carry out because with the impact energy increase, numerous new scattering channels become opened, and more detailed scattering data around the TCS maximum are not available as yet.

Above 12 eV the measured  $e^-$ -SO<sub>2</sub>Cl<sub>2</sub> TCS energy function decreases rather monotonically down to  $24 \times 10^{-20} \text{ m}^2$  at 150 eV, the highest applied energy. Our computations show (figure 1) that the shape and magnitude of the experimental TCS at intermediate energies (more precisely between 70 and 150 eV) are satisfactorily reproduced by the sum of the calculated elastic and ionization electron-scattering cross sections, and indicate that at intermediate energies these two processes dominate the  $e^-$ -SO<sub>2</sub>Cl<sub>2</sub> scattering. Taking into account that computations we have performed hitherto for other polyatomic targets agree fairly well with observations above 70 eV, we suppose that the present calculations also represent *true* intermediate-energy electron-scattering TCS adequately. Below 70 eV, however, as the energy decreases, the computations become more and more higher than the measurements (figure 1). This is mainly due to inadequacy of the independent atom approximation for an appropriate description of elastic scattering at low energies. At these energies, the wavelength of the impinging electron becomes comparable with the molecular size and the screening effects should be taken into consideration (cf [51, 52]).

#### 4.2. Comparison with other SO<sub>2</sub>-containing molecules

Figure 2 summarizes the experimental TCS results for sulfone derivatives (SO<sub>2</sub>Cl<sub>2</sub>, SO<sub>2</sub>ClF and SO<sub>2</sub>F<sub>2</sub>) together with measurements for a SO<sub>2</sub> molecule. The TCS measurements for SO<sub>2</sub>Cl<sub>2</sub> (present), SO<sub>2</sub>ClF [34] and SO<sub>2</sub> [29] were taken in our laboratory, while those for SO<sub>2</sub>F<sub>2</sub>—available only at low energies—come from an outer source [33]; unfortunately, due to some regulations, we could not purchase the SO<sub>2</sub>F<sub>2</sub> sample. The total cross sections

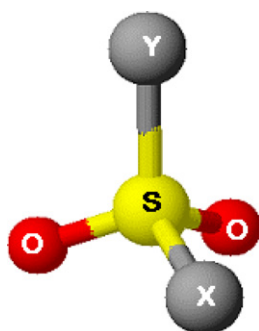


**Figure 3.** A schematic diagram of SO<sub>2</sub>XY (X,Y = Cl,F) molecular geometry. For values of interatomic distances and angles, see table 3.

**Table 4.** Ionization (ICS), integral elastic (ECS) and *total* (ICS + ECS) cross sections calculated for electron impact on a SO<sub>2</sub>F<sub>2</sub> molecule (in units of 10<sup>-20</sup> m<sup>2</sup>).

Energy (eV)	ICS	Energy (eV)	ICS	ECS	Total	Energy (eV)	ICS	ECS	Total
		40	3.93	29.0	32.9	250	5.43	8.68	14.1
13.597	0.0	45	4.42	26.2	30.6	300	5.04	7.82	12.9
14.0	0.0154	50	4.82	24.0	28.8	350	4.70	7.14	11.8
15.0	0.0901	60	5.42	20.8	26.2	400	4.40	6.60	11.0
16.0	0.201	70	5.82	18.6	24.4	450	4.13	6.14	10.3
17.0	0.342	80	6.07	16.9	23.0	500	3.89	5.75	9.64
18.0	0.503	90	6.22	15.7	21.9	600	3.49	5.12	8.61
19.0	0.663	100	6.31	14.7	21.0	700	3.17	4.62	7.79
20.0	0.819	110	6.34	13.8	20.2	800	2.90	4.23	7.13
22.5	1.25	120	6.34	13.1	19.5	900	2.68	3.90	6.58
25.0	1.72	140	6.27	12.0	18.3	1000	2.49	3.62	6.11
27.5	2.18	160	6.15	11.2	17.3	2000	1.49	2.20	3.69
30.0	2.61	180	6.00	10.4	16.4	3000	1.08	1.71	2.79
35.0	3.34	200	5.84	9.84	15.7	4000	0.854	1.59	2.44

computed in the present work for these compounds are also shown in figure 2 for comparison. The computed cross sections for SO<sub>2</sub>F<sub>2</sub> are listed in table 4. Figure 3 illustrates the geometry of sulfone-containing molecules under study; they all have distorted tetrahedral configuration with the sulfur atom located in the centre.

With respect to the shape, the low-energy part of the measured TCS for SO<sub>2</sub>Cl<sub>2</sub> closely resembles the behaviour of TCS for SO<sub>2</sub>CIF [34]. The minimum and both neighbouring shoulders visible in the e<sup>-</sup>-SO<sub>2</sub>Cl<sub>2</sub> TCS function are, however, shifted towards lower energies by about 1 eV while location of the maximum in both curves is the same, about 9.5 eV. Between 20 and 40 eV, the curves for SO<sub>2</sub>Cl<sub>2</sub> and SO<sub>2</sub>CIF distinctly differ; the TCS for SO<sub>2</sub>CIF has a broad shoulder (attributed to the presence of fluorine atom) while the SO<sub>2</sub>Cl<sub>2</sub> function monotonically decreases. There is also a weak similarity between the SO<sub>2</sub>Cl<sub>2</sub> curve and the SO<sub>2</sub>F<sub>2</sub> curve [33], over the energy range where both were measured. Surprisingly, at low energies there is a much better likeness with regard to the shape of the TCS curves for SO<sub>2</sub>F<sub>2</sub> and SO<sub>2</sub>. Such a close similarity of both curves indicates that addition of fluorine atoms to a SO<sub>2</sub> molecule influences the shape of the low-energy TCS much less than addition of chlorine.

In view of the TCS magnitude, over the whole energy range investigated, the experimental and theoretical TCS values for sulfone derivatives follow their geometrical size; the larger the molecule (cf table 3), the higher the TCS value. There are some indications, however, that the TCS for SO<sub>2</sub>F<sub>2</sub> [33] is distinctly underestimated (by about 20–30%). Support for such a conclusion arises from a comparison of TCS behaviour for fluorinated targets and from the fact that experimental data for other targets (e.g. CHF<sub>3</sub>, CF<sub>4</sub>, c-C<sub>4</sub>F<sub>8</sub>), obtained in the same laboratory where SO<sub>2</sub>F<sub>2</sub> data were taken, are systematically lower than those of other groups (for references, see [53]). On the other site, it is interesting that transparency of SO<sub>2</sub>F<sub>2</sub> at low energies is much higher, nearly twice, than that of a SO<sub>2</sub> molecule.

## 5. Summary

In this paper we reported the absolute *grand* total cross section (TCS) for 0.5–150 eV electrons scattered by SO<sub>2</sub>Cl<sub>2</sub> molecules measured using a linear transmission method. In the low-energy range some features in the TCS are discernible which can be explained through resonant processes. Generally, the shape of the e<sup>-</sup>-SO<sub>2</sub>Cl<sub>2</sub> TCS is very similar to that of SO<sub>2</sub>ClF, except for energies between 20 and 40 eV. Our calculated intermediate-energy total (elastic + ionization) cross section reproduces quite satisfactorily the experimental e<sup>-</sup>-SO<sub>2</sub>Cl<sub>2</sub> TCS data between 70 and 150 eV. Such a good agreement between experiment and theory lets us to believe that above 150 eV, the calculated cross section reasonably complements the measured TCS values. A comparison of e<sup>-</sup>-SO<sub>2</sub>XY (X,Y = Cl,F) data suggests that measurements available for SO<sub>2</sub>F<sub>2</sub> [33] are significantly underestimated. Some similarities and differences between TCS for sulfone derivatives are pointed out; however, lack of experimental electron-scattering data for a SO<sub>2</sub>F<sub>2</sub> molecule over a wider energy range makes impossible more definite statements on the role of molecular configuration in the scattering. Therefore, additional more detailed experiments for this family of molecules are encouraged as well as low-energy calculations.

## Acknowledgments

The work is a part of research programme sponsored by the Ministry of National Education and Science (MEiN) and the Ministry of Scientific Research and Information Technology (MNiI). Numerical calculations have been performed at the Academic Computer Center in Gdańsk (TASK).

## References

- [1] Yu G, Mason H J, Wu X, Endo M, Douglas J and Macor J E 2001 *Tetrahedron Lett.* **42** 3247–9
- [2] Alonso M and Riera A 2005 *Tetrahedron: Asymmetry* **16** 3908–12
- [3] Boyle T J, Andrews N L, Alam T M, Tallant D R, Rodrigues M A and Ingersoll D 2005 *Inorg. Chem.* **44** 5934–40
- [4] DeMore W B, Leu M-T, Smith R H and Yung Y L 1985 *Icarus* **63** 347–53
- [5] Rosenbaum O and Neuert H 1954 *Z. Naturforschg. A* **9** 990–1
- [6] Sullivan S A and Beauchamp J L 1978 *Int. J. Mass Spectrom. Ion Phys.* **28** 69–80
- [7] Robbiani R and Franklin J L 1979 *J. Am. Chem. Soc.* **101** 3709–15
- [8] Wang J-S and Franklin J L 1980 *Int. J. Mass Spectrom. Ion Phys.* **36** 233–47
- [9] Beale J, Armitage S and Laricchia G 2006 *J. Phys. B: At. Mol. Opt. Phys.* **39** 1337–44
- [10] Brüche E 1930 *Ann. Phys., Lpz.* **4** 387–408
- [11] Floeder K, Fromme D, Raith W, Schwab A and Sinapius G 1985 *J. Phys. B: At. Mol. Phys.* **18** 3347–59
- [12] Nishimura H and Tawara H 1991 *J. Phys. B: At. Mol. Opt. Phys.* **24** L363–6
- [13] Szmytkowski Cz, Możejko P and Kasperski G 1998 *J. Phys. B: At. Mol. Opt. Phys.* **31** 3917–28
- [14] Kimura M, Sueoka O, Hamada and Itikawa Y 2000 *Adv. Chem. Phys.* **111** 537–622

- [15] Lopes A R, Bettega M H F, Lima M A P and Ferreira L G 2004 *J. Phys. B: At. Mol. Opt. Phys.* **37** 997–1012
- [16] Szymtkowski Cz and Kwitniewski S 2002 *J. Phys. B: At. Mol. Opt. Phys.* **35** 2613–23, 3781–90
- [17] Szymtkowski Cz and Kwitniewski S 2003 *J. Phys. B: At. Mol. Opt. Phys.* **36** 2129–38, 4865–73
- [18] Makochekanwa C, Kato H, Hoshino M, Cho H, Kimura M, Sueoka O and Tanaka H 2005 *Eur. Phys. J. D* **35** 249–55
- [19] Kasperski G, Możejko P and Szymtkowski Cz 1997 *Z. Phys. D* **42** 187–91
- [20] Szymtkowski Cz, Możejko P, Kasperski G and Ptasieńska-Denga E 2000 *J. Phys. B: At. Mol. Opt. Phys.* **33** 15–22
- [21] Szymtkowski Cz and Ptasieńska-Denga E 2001 *Vacuum* **63** 545–8
- [22] Szymtkowski Cz, Możejko P and Kwitniewski S 2002 *J. Phys. B: At. Mol. Opt. Phys.* **35** 1267–74
- [23] Szymtkowski Cz, Kwitniewski S, Możejko P and Ptasieńska-Denga E 2002 *Phys. Rev. A* **66** 014701
- [24] Szymtkowski Cz, Kwitniewski S and Ptasieńska-Denga E 2003 *Phys. Rev. A* **68** 032715
- [25] Szymtkowski Cz, Domaracka A, Możejko P, Ptasieńska-Denga E, Kłosowski Ł, Piotrowicz M and Kasperski G 2004 *Phys. Rev. A* **70** 032707
- [26] Szymtkowski Cz, Piotrowicz M, Domaracka A, Kłosowski Ł, Ptasieńska-Denga E and Kasperski G 2004 *J. Chem. Phys.* **121** 1790–5
- [27] Szymtkowski Cz and Możejko P 2001 *Vacuum* **63** 549–54
- [28] Knudsen M 1910 *Ann. Phys., Lpz.* **31** 205–29
- [29] Szymtkowski Cz, Możejko P and Krzysztofowicz A 2003 *Rad. Phys. Chem.* **68** 307–11
- [30] Gullett R J, Field T A, Steer W A, Mason N J, Lunt S L, Ziesel J-P and Field D 1998 *J. Phys. B: At. Mol. Opt. Phys.* **31** 2971–80
- [31] Makochekanwa C, Kawate H, Sueoka O and Kimura M 2003 *J. Phys. B: At. Mol. Opt. Phys.* **36** 1673–80
- [32] Makochekanwa C, Sueoka O and Kimura M 2003 *J. Chem. Phys.* **119** 12257–63
- [33] Wan H-X, Moore J H, Olthoff J K and van Brunt R J 1993 *Plasma Chem. Plasma Process.* **13** 1–16
- [34] Szymtkowski Cz, Możejko P, Kwitniewski S, Ptasieńska-Denga E and Domaracka A 2005 *J. Phys. B: At. Mol. Opt. Phys.* **38** 2945–54
- [35] Możejko P, Żywicka-Możejko B and Szymtkowski Cz 2002 *Nucl. Instrum. Methods Phys. Res. B* **196** 245–52
- [36] Możejko P and Sanche L 2005 *Rad. Phys. Chem.* **73** 77–84
- [37] Szymtkowski Cz, Domaracka A, Możejko P, Ptasieńska-Denga E and Kwitniewski S 2005 *J. Phys. B: At. Mol. Opt. Phys.* **38** 745–55
- [38] Hwang W, Kim Y K and Rudd M E 1996 *J. Chem. Phys.* **104** 2956–66
- [39] Frisch M J *et al* 2003 *GAUSSIAN 03*, Revision B.05 (Pittsburgh: Gaussian, Inc.)
- [40] Zakrzewski V G and von Niessen W 1994 *J. Comput. Chem.* **14** 13–8
- [41] Kim Y-K, Hwang W, Weinberger N M, Ali M A and Rudd M E 1997 *J. Chem. Phys.* **106** 1026–33
- [42] Basner R, Schmidt M, Deutsch H, Tarnovsky V, Levin A and Becker K 1995 *J. Chem. Phys.* **103** 211–8
- [43] Lindsay B G, Straub H C, Smith K A and Stebbings R F 1996 *J. Geophys. Res.* **101** 21151–6
- [44] Mott N F and Massey H S W 1965 *The Theory of Atomic Collisions* (Oxford: Oxford University Press)
- [45] Salvat F, Martinez J D, Mayol R and Parellada J 1987 *Phys. Rev. A* **36** 467–74
- [46] Padiyal N T and Norcross D W 1984 *Phys. Rev. A* **29** 1742–8
- [47] Zhang X, Sun J and Liu Y 1992 *J. Phys. B: At. Mol. Opt. Phys.* **25** 1893–8
- [48] Lide D R (ed) 2004–2005 *CRC Handbook of Chemistry and Physics* 85th edn (Boca Raton, FL: CRC Press)
- [49] Müller H S P and Gerry M C L 1994 *J. Chem. Soc. Faraday Trans.* **90** 2601–10
- [50] Szymtkowski Cz 1989 *Z. Phys. D* **13** 69–73
- [51] Sun J-F, Du Ch-L and Liu Y-F 2003 *Phys. Lett. A* **314** 150–5
- [52] Sun J-F, Du Ch-L, Shi D-H and Liu Y-F 2004 *Chin. Phys.* **13** 1418–22
- [53] Christophorou L G and Olthoff J K 2004 *Fundamental Electron Interactions with Plasma Processing Gases* (New York: Kluwer/Plenum)